REGIOCHEMISTRY OF SINGLET OXYGEN ENE REACTION IN METAL-ORGANIC FRAMEWORKS

A Thesis

Presented to

The Faculty of the Department of Chemistry and Biochemistry

California State University, Los Angeles

In Partial Fulfillment

of the Requirements for the Degree

Master of Science

in

Chemistry

By

Jin Hyeok Yoon

August 2023

© 2023

Jin Hyeok Yoon

ALL RIGHTS RESERVED

The thesis of Jin Hyeok Yoon is approved.

Matthias Selke, Ph.D., Committee Chair

Yangyang Liu, Ph.D.

Yixian Wang, Ph.D.

Krishna Foster, Ph.D., Department Chair

California State University, Los Angeles

August 2023

ABSTRACT

Regiochemistry of Singlet Oxygen Ene-Reaction in Metal Organic Frameworks.

By

Jin Hyeok Yoon

Photooxidation of olefins leading to allylic hydroperoxides is a versatile reaction with various synthetic applications. However, when carried out in homogeneous media, this reaction's potential is limited due to its intermediate yielding several different regioisomeric products. While zeolites have been used to control the selectivity with modest success, other stable and versatile materials have not been investigated as heterogenous catalyst for the singlet oxygen ene reaction.

In this study, we utilized metal-organic frameworks (MOFs) to study the singlet oxygen ene reaction. MOFs can produce singlet oxygen in good yield, and they may be used to provide a sterically constrained environment to potentially control product selectivity in the ene reaction. To our knowledge, this is the first study of the singlet oxygen ene reaction in a metal-organic framework. Several different MOFs were investigated namely aluminum-Tetrakis Carboxyl Phenyl Porphyrin (Al-TCPP), Daegu Gyeongbuk Institute of Science and Technology (DGIST-1), and Nanjing University Porphyrinic Framework no.2 Yttrium (NUPF-2Y). The results showed that Al-TCPP and DGIST-1 did have a modest effect on the selectivity of the reaction. However, the reaction time varies considerably depending on the MOF used: While Al-TCPP required 30 minutes to complete the reaction, NUPF-2Y and DIGST-1 required prolonged radiation to fully convert the olefins to the corresponding allylic hydroperoxides. Lastly, comparison between Al-TCPP and NUPF-2Y results suggests that the MOF's topology may be more significant than the MOFs' pore parameters. Overall, this study has demonstrated the

MOF's potential as photocatalysts for the singlet oxygen ene reaction. Further studies are required to find optimal conditions to obtain only to affect the reaction's selectivity.

ACKNOWLEDGMENTS

I would like to acknowledge my advisors Dr. Selke and Dr. Liu for their guidance and mentorship to help me grow as a chemist and a leader. Additionally, I would like to send my thanks to the chemistry department and the staff for supporting us throughout the project.

Lastly, I would also like to acknowledge the financial support from the Army Research Office (Grant Number W911NF-19-1-0001) and the National Science Foundation CREST program (HRD 1547723).

TABLE OF CONTENTS

Abstract iv

Acknowledgments vi

List of Tables ix

List of Figures x

Chapters

1. The Singlet Oxygen Ene Reaction: Scope and Limitations 1

2. Synthesis and Characterization of Metal Organic Frameworks (MOFs) for Singlet Oxygen Ene Chemistry 6

2.1 Instrumentation 6

2.2 Synthesis of Al-TCPP 6

2.3 Synthesis of DGIST-1 7

2.3.1. $Ti_6O_6(O^iPr)_6(t\text{-}BA)_6$ cluster 7

2.3.2. DGIST-1 7

2.4 Synthesis of NUPF-2Y 8

2.5 MOF Characterization 9

2.6 Materials 11

3. The Singlet Oxygen Ene Reaction in Metal-Organic Frameworks: Regiochemistry and Yield 12

3.1. Materials and Methods: 12

3.1.1 Photooxidation of 2-Methyl-2-Heptene in MOFs: General Procedure 12

3.1.2. UV-Vis Spectrometer Soret Band 14

3.2. Photooxidation of 2-Methyl-2-Heptene in Three Different MOFs: Product

Selectivity and Reaction Time 14

4. The Singlet Oxygen Ene Reaction: Findings and the Future 18

References 19

Appendices:

A. ^{1}HNMR of photooxidation with TCPP in CD_3CN 23

B. ^{1}HNMR of photooxidation with TCPP in CD_3OD 23

C. ^{1}HNMR of photooxidation with Al-TCPP in CD_3CN 24

D. ^{1}HNMR of photooxidation with Al-TCPP in CD_3OD 24

E. ^{1}HNMR of photooxidation with DGIST-1 in CD_3CN 25

F. ^{1}HNMR of photooxidation with NUPF-2Y in CD_3CN 25

G. ^{1}HNMR of photooxidation with NUPF-2Y in CD_3OD 26

LIST OF TABLES

Table

1. Summary of MOF Characterization.....10

2. Summary of Photooxidation of 2-Methyl-2-Heptene in TCPP and MOFs. 15

LIST OF FIGURES

Figures

1. Overview of Photosensitization 2

2. Hydrogen Abstraction Step from the perEpoxide Intermediate 2

3. Photooxidation of 2-Methyl-2-Heptene Yields Two Distinct Products 3

4. Photooxidation of 2-Methyl-2-Pentene in the Y Zeolite 4

5. Synthesis of Al-TCPP 7

6. Synthesis of DGIST-1 8

7. Synthesis of NUPF-2Y 9

8. Powder X-ray Diffraction Spectra of (a)Al-PMOF, (b) DGIST-1, (c) NUPF-2Y, and N_2 Adsorption and Isotherms of (d)Al-PMOF, (e) DGIST-1, (f) NUPF-2Y 10

9. UV-Vis spectra of TCPP, Al-PMOF, DGIST-1, and NUPF-2Y 11

10. ^{1}HNMR of the Reactant 13

11. ^{1}HNMR of Product 2a 13

12. ^{1}HNMR of Product 2b 13

13. The Summary of Photooxidation of 2-Methyl-2-Heptene.....15

14. Topology of Al-TCPP, DGIST-1, NUPF-2Y 16

CHAPTER 1

The Singlet Oxygen Ene Reactions: Scope and Limitations

The singlet oxygen ene-reaction is one of the essential methods to introduce oxygen functionality into organic compounds.[1-3] Schenck's group first reported that this reaction yields allylic hydroperoxide products.[4] As one of the essential components in the reaction, singlet oxygen is an excited reactive oxygen species generated through a pathway called photosensitization.[1,3,5] In this pathway, the ground state of a light-absorbing dye called photosensitizer (*PSs*) absorbs photons to become an excited singlet state of photosensitizer (^1PSs). Following the excitation, ^{1}PSs quickly undergo inter-system crossing (ISC) to yield ^{3}PSs, which proceeds to either a: (i) Type 1 reaction to produce radicals or, (ii) Type 2 reaction to generate singlet oxygen ($^1O_2$). Singlet oxygen is generated during the collision between the ground state ^{3}PSs and ground-state molecular oxygen with energy transfer (Figure 1**)**. Due to its degenerate HOMO and LUMO orbitals, singlet oxygen is a strong oxidant and readily reacts with organic molecules and heteroatoms; and it is an environmentally benign oxidant since it is generated from light and molecular O_2.[3,5] Since the discovery of photochemical singlet oxygen generation by Foote and Wexler in 1964,[6] various studies have been performed to understand the scope and mechanism of singlet oxygen reactions with organic substrates and heteroatoms.[1]

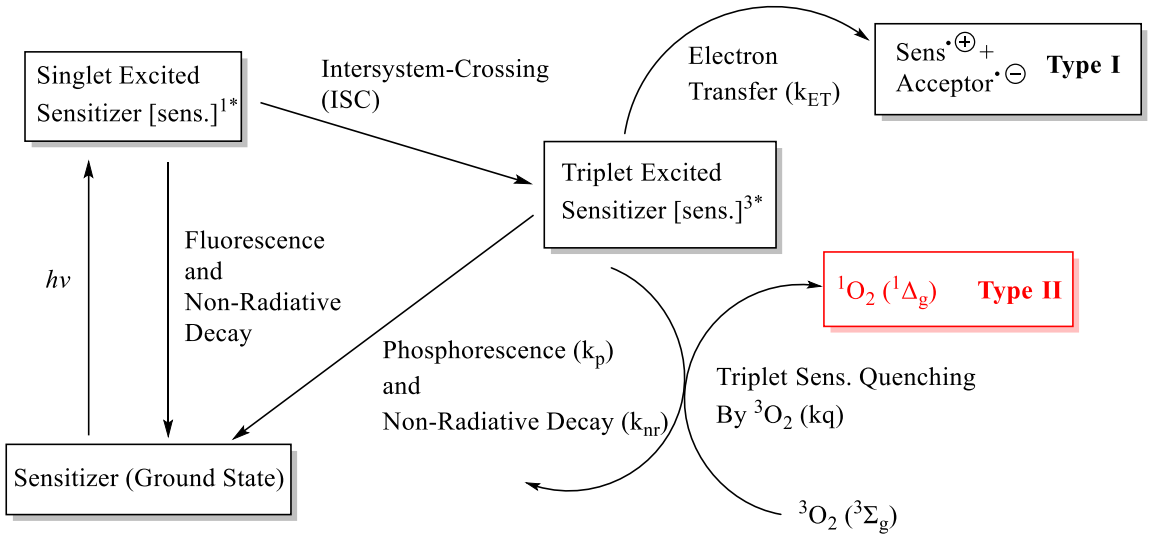


Figure 1. The overview of photosensitization leading to Type 1 and Type 2 reactions to yield radicals and singlet oxygen, respectively.[3,5]

One of the most prominent applications of singlet oxygen chemistry is the photooxidation of olefins to synthesize allylic hydroperoxide products, which can further reduce to allylic alcohols. Although this concept is widely used in drug synthesis and investigation of natural products,[1,6,7] the singlet oxygen ene-reaction has limited synthetic applications due to triangular peroxidic intermediate: Foote et al. demonstrated that the electronegative oxygen in the intermediate abstracts hydrogen from two different positions (Figure 2), leading to two distinct regioisomers.[9]

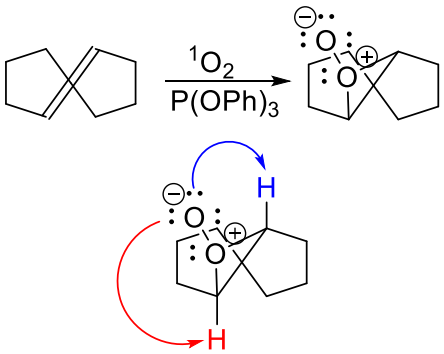


Figure 2. Hydrogen abstraction step from the perepoxide intermediate. The formation of reactive perepoxide intermediate undergoes two different hydrogen atom abstractions to yield two regioisomers evenly.[9]

Various experiments using different materials have been performed to utilize this reaction. The Orfanopoulous group studied the photooxidation of 2-methyl-2-heptene in the presence of C_{60} fullerene with aluminum or silicon supporting surfaces in aprotic and protic solvents (Figure 3).[10] They observed: (i) higher conversion percentage from the reactant (1 in Figure 3) to the products (2a and 2b in Figure 3) in the deuterated solvents, which increased the lifetime of singlet oxygen[1,10]; (ii) The potential to control the selectivity using different supporting surfaces.[7]

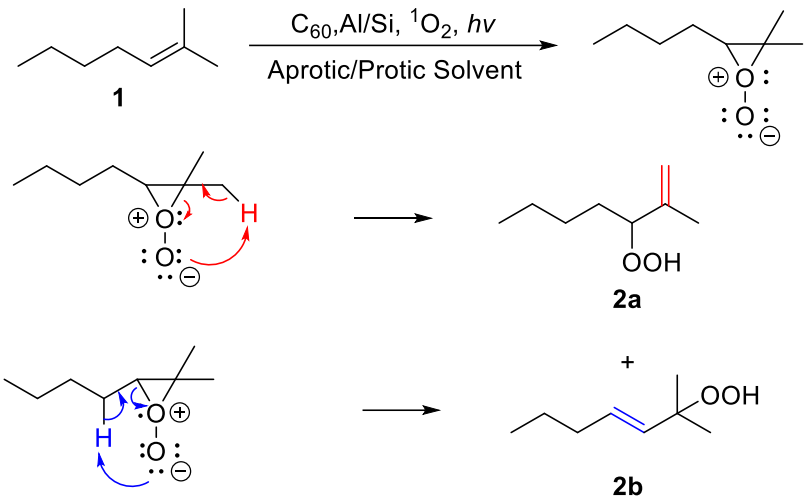


Figure 3. Photooxidation of 2-methyl-2-heptene using C_{60} fullerene with silica and γ-alumina in acetonitrile, dimethyl sulfoxide, deuterium oxide, hexanes, methanol, and water.[10]

In addition to Orfanopoulos's work, Li et al. investigated this reaction using Y-zeolite.[11] From their work, Li et al. reported that the control group with thionine methylene blue, a photosensitizer, yielded 40% of product 1a and 60% of product 1b in acetonitrile. However, the reaction resulted in a single primary product of 1a (Figure 4) in the presence of Y zeolite.[11] Li et al. stated that the small pores of the Y-zeolite prevented a free rotation of carbon-carbon $\boldsymbol{\sigma}$ bonds (green bond in Figure 4) while making the methylene hydrogen closer to the peroxide intermediate, thus yielding a 2b product.[10,11] Even though previous studies have shown the potential to control the selectivity of the reaction, there are limitations to using zeolite. For

instance, because a zeolite experiment requires separate photosensitizers to generate singlet oxygen, which is slowly photobleached under prolonged irradiation.[4] Furthermore, zeolites are considered inadequate for bulky substrates and may undergo irreversible deactivation during reactions, attributed to the reactant's incomplete conversion rate.[13-15] Therefore, a novel approach using a stable and versatile material would be a significant improvement as far as the utility of this process is concerned.

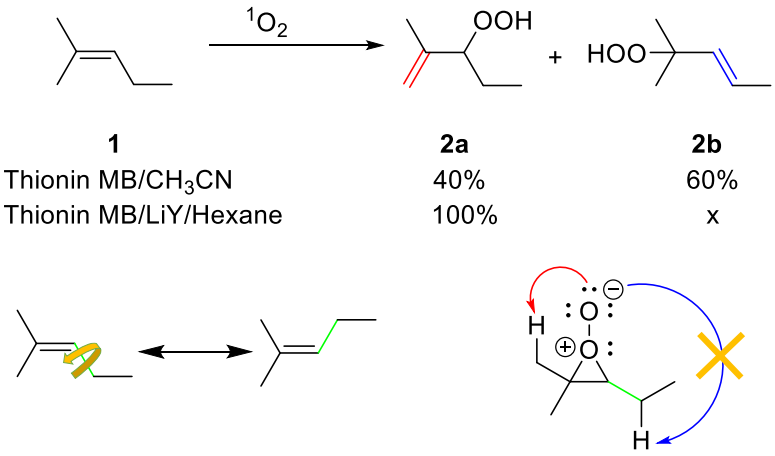


Figure 4. Photooxidation of 2-methyl-2-pentene using a Y-zeolite containing oxazine and thiazine dye molecules in acetonitrile and hexane. Samples were irradiated for 30 minutes and analyzed using gas chromatography. The carbon-carbon σ bonds in green can rotate freely in a free solution. However, this rotation is prohibited in the Y-zeolite due to the steric hindrance, thus preventing the methylene hydrogen abstraction.[11]

As a potential candidate, metal-organic frameworks are crystalline structures of porous materials consisting of metal nodes and organic linkers.[16] Because of its nearly limitless combinations and various synthesis procedures, there are approximately 900,000 MOFs for various applications.[17] As photocatalysts, frameworks with porphyrins have been reported to generate singlet oxygen by harvesting energy through the aromatic systems as do free porphyrins.[18-21] Furthermore, a previous study has demonstrated that the MOFs' confinement, such as pore diameter and surface area, may form different products. In Hemmer's article, the group learned that utilizing MOFs with bigger pore diameters yielded a complex cross-linked

polymer. However, in the presence of a MOF with a smaller pore diameter, the same reactant resulted in a simpler polymer due to steric hindrance.[22]

Based on the previous experiments, a novel approach to studying this reaction's selectivity in the presence of MOFs. With porphyrin linkers and various metal nodes, these frameworks can generate singlet oxygen and yield a significant product.[18-21] We hypothesized that MOFs might lead to the preferential formation of one of the two ene-reactions due to the restricted size of the cavity where the reaction occurs. Therefore, we used Al, Ti, and Y MOFs with different pore parameters to study the selectivity of the singlet oxygen ene-reaction.

CHAPTER 2

Synthesis and Characterization of Metal Organic Frameworks (MOFs) for Singlet Oxygen Ene Chemistry

2.1 Instrumentation

We obtained Powder X-ray diffraction (PXRD) spectrums by placing the MOF samples on a D2 Phaser equipped with a Cu-sealed tube ($\lambda = 1.54178$) at 30 kV and ten mA over a range of 2-30° with a step size of $2\theta = 0.01°$ (1 second per step). Then we obtained MOFs' Brunauer-Emmett-Teller (BET) surface areas and the pore distribution using Micromeritics ASAP 2020 Plus. We used a Shimadzu UV-2600 spectrophotometer with ISR-2600 integrating sphere using 1 cm light path quartz cuvettes to obtain the UV-vis spectra. For the photooxidation reactions, we fabricated the LED irradiation setup by mounting LEDs purchased from RapidLED into an aluminum base. We then connected the LEDs in series to a Mean Well LPC-35-700 constant current driver purchased from RapidLED. In an aluminum base, we placed four CREE XT-E Royal Blue LEDs facing each other approximately 3 cm apart. The power density of each blue LED is 200 mW/cm2. Lastly, we obtained the ^{1}H NMR spectra using Bruker 400 MHz NMR spectrometer.[23]

2.2 Synthesis of Al-TCPP

The Al-TCPP was synthesized following the literature reported by Fateeva's group.[24] In a 20ml Teflon line autoclave reactor, 0.126 mmol of 5,10,15,20-tetrakis (4-carboxyphenyl) porphyrin (TCPP), and 0.25 mmol of $AlCl_3 \cdot 6H_2O$ were mixed with 10 mL of deionized water. After sonicating the suspension for 10 minutes, the Teflon container was placed into the autoclave steel reactor and heated to 160 °C for 16 hours in a programmable oven. The solution was cooled at a rate of 1.5 °C/ minute until reaching room temperature. The powder was

collected from centrifugation and washed with DMF and acetone three times each. After washing, the powder was dried in the vacuum oven at room temperature overnight, and a red powder was obtained (Yield: 36%).

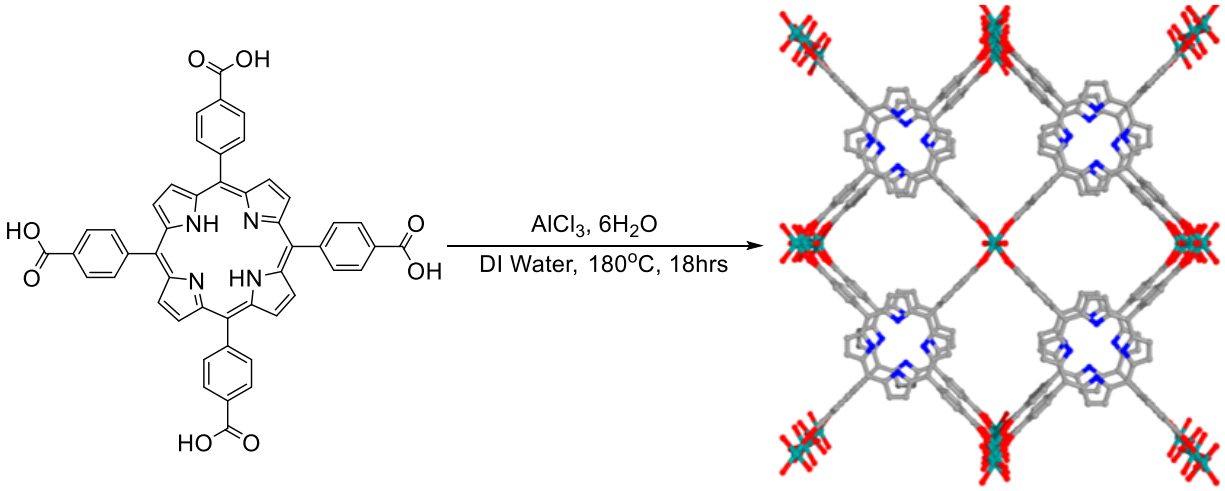


Figure 5. Al-TCPP was synthesized with aluminum chloride hexahydrate and Meso-tetra(4-carboxyphenyl) porphyrin (TCPP).[23,24]

2.3 Synthesis of DGIST-1

2.3.1. $Ti_6O_6(O^iPr)_6(t\text{-}BA)_6$ cluster.

We synthesized the cluster by adding 7.5mmol of 3,3-dimethyl butyric acid dropwise to a solution containing: 1mmol of Mn $(NO_3)_2 \cdot 4H_2O$, and 2.75ml of isopropyl alcohol. After stirring for 20 minutes, the solution was capped in a 40 mL glass test tube and heated to 80 °C for 24 hours. The white crystal products were washed three times with isopropyl alcohol and acetone and then dried at 60 °C under vacuum overnight (Yield:36%).[25]

2.3.2. DGIST-1.

The Ti-MOF was synthesized following the literature reported by Keum's group with a minor modification.[24] In a 35 mL glass pressure vial, 60 mg of $Ti_6O_6(O^iPr)_6(t\text{-}BA)_6$, 300 mg of TCPP, and 2g of benzoic acid were dissolved in 20 mL of DMF. The solution was mixed and sonicated for 20 minutes, then placed in the oven at 150 °C for 72 hours. The resulting reddish-

purple crystals were washed nine times with DMF over three days, followed by six additional times with acetone in one day. The resulting powder was dried in the gas adsorption tube via the Schlenk line for 2 hours (Yield: 37%).

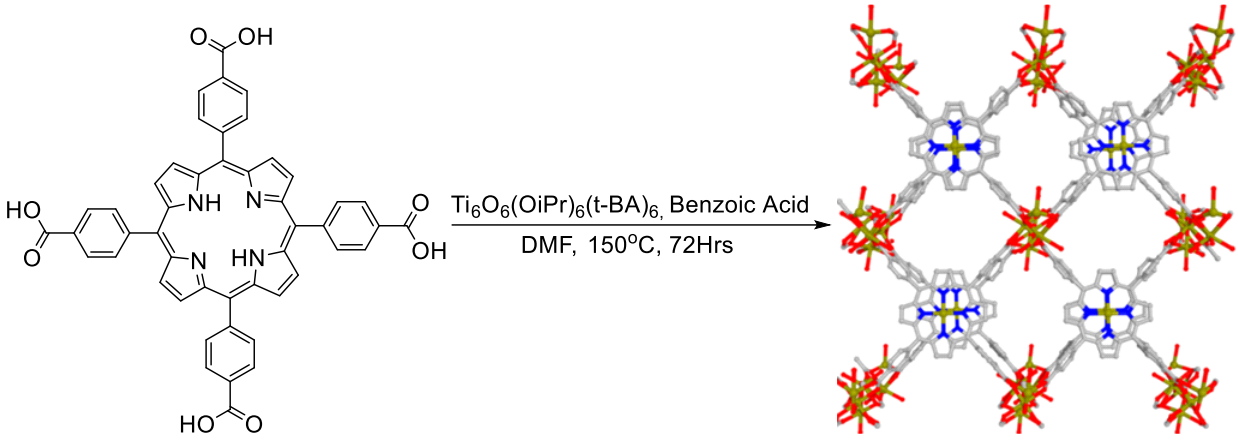


Figure 6. DGIST-1 was synthesized with $Ti_6O_6(O^iPr)_6(t\text{-}BA)_6$ cluster, meso-tetra(4-carboxyphenyl) porphyrin (TCPP), and benzoic acid as a modulator.[23,25] Additionally, we placed the sample in the oven for additional 24 hours to increase the yield.

2.4 Synthesis of NUPF-2Y

NUPF-2Y was synthesized following the literature reported by Xu's group.[26] Three hundred and eighty milligrams of $Y(NO_3)_3{\cdot}6H_2O$, hundred milligrams of TCPP, one gram of 2-fluorobenzoic acid as a modulator, twenty milliliters of DMF, and five milliliters of DI water were added to an autoclave Teflon container. The solution was sonicated for 15 minutes, inserted into the autoclave steel reactor, and heated to 120 ºC for 72 hours. The reactor was cooled to room temperature, and the crystalline product was washed three times with DMF, twice with anhydrous ethanol, and once with DCM. The dark purple product was dried in a vacuum oven for 1 hour at room temperature (Yield: 53%).

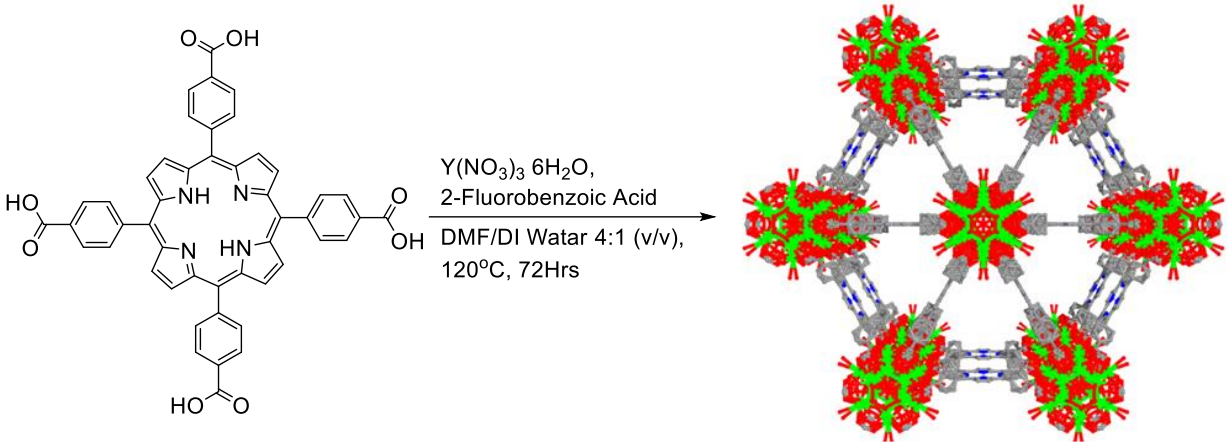


Figure 7. NUPF-2Y was synthesized with yttrium (III) nitrate hexahydrate, meso-tetra(4-carboxyphenyl) porphyrin (TCPP), and 2-fluorobenzoic acid as a modulator.[23,26]

2.5 MOF characterization

We analyzed Al-TCPP, DGIST-1, and NUPF-2Y using PXRD, N2 adsorption, and isotherm to investigate the regiochemistry of the singlet oxygen ene reaction. As shown in Figure 8, the results from PXRD demonstrated that the experimental peaks matched the literature values, indicating that the lattice crystalline structure matched. However, we also observed a few minor differences. In Figure 8-2b, the peak near nine 2θ had a different pattern because the MOF favored a more stable structure while the instrument examined the powder in a solvent-free condition. After confirming the lattice crystalline structure, we activated the MOFs using N2 adsorption and isotherm instruments. During the activation process, any remaining solvent residue in the MOFs was removed at a high temperature and then filled with N2 gas. Once fully activated, MOFs' details, such as surface area and pore diameter, were calculated from the isotherm instrument by using the density functional theory (DFT). As shown in Table 1, the data showed that the porous MOFs with the desired pore diameter and surface area were successfully synthesized.

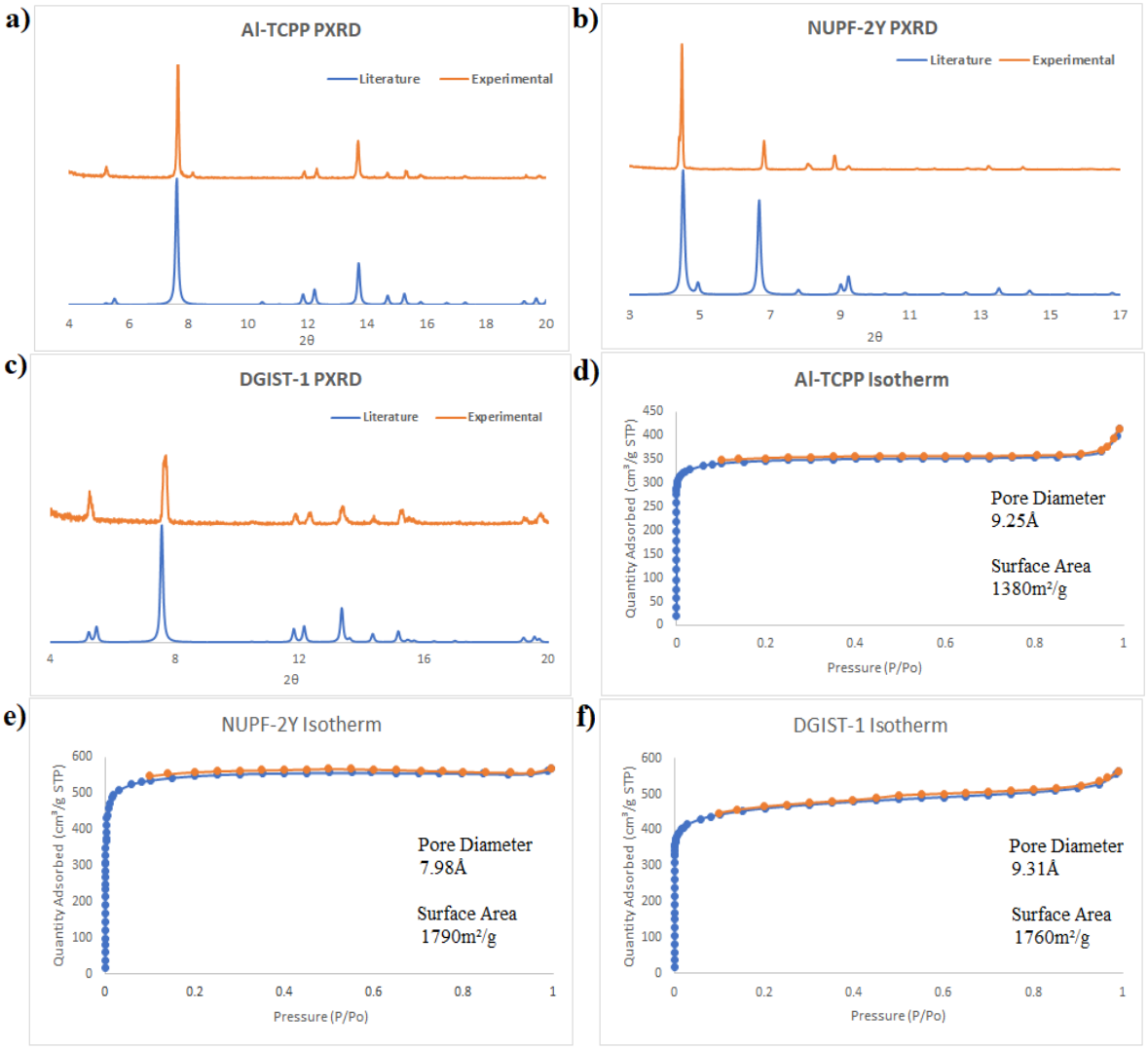


Figure 8. Powder X-Ray Crystallography pattern of a). Al-TCPP b). NUPF-2Y c). DGIST-1 showed that the experimental peaks (orange) matched the simulated peaks (blue). However, a minor difference was observed near nine 2θ in NUPF-2Y due to the position of the powder; NUPF-2Y may favor a specific configuration while being tested. After confirming the general crystalline structure, the N_2 adsorption and isotherm of d). Al-TCPP e). NUPF-2Y f). DGIST-1 indicated that the desired MOFs were synthesized.[24-26]

MOFs	Al-TCPP	DGIST-1	NUPF-2Y
Pore Diameter (Å)	8.19-9.63	9.31-9.95	7.98-8.76
Surface Area (m^2/g)	1140-1630	1550-1760	1470-1790

Table 1. MOFs were synthesized and characterized using PXRD, N_2 adsorption, and the isotherm. The pore diameter and the surface area indicate the ranges of the MOFs that has been successfully synthesized.[24-26]

In addition to characterizing MOFs, we investigated the absorption spectra of the MOFs.

Using the UV-vis spectrometer equipped with an integrating sphere, we obtained the soret bands of the photosensitizers shown in Figure 9. The result indicates that every photosensitizer had soret bands between 410nm and 450nm, which falls within the range of the blue LED light. From this result, TCPP and the desired MOFs can generate singlet oxygen under the energy source.

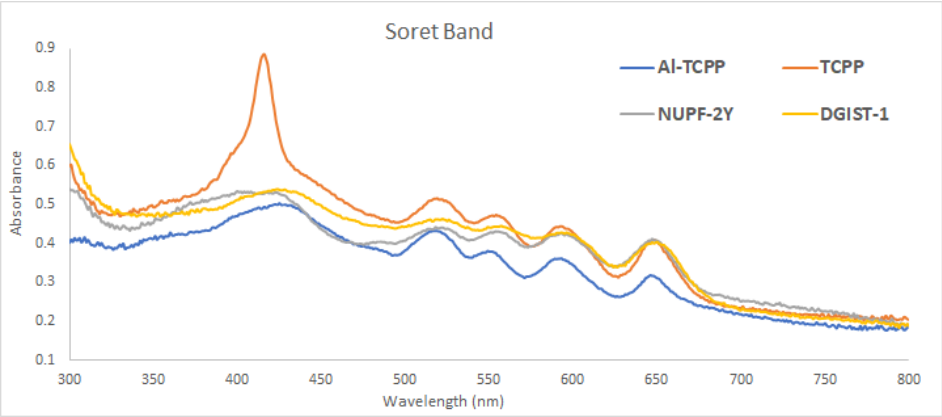


Figure 9. The UV-vis spectra were obtained using the UV-Vis spectrometer equipped with an integrating sphere. The samples were prepared in the chloroform, sonicated for 5 minutes, and diluted until the initial concentration fell between 0.180 and 2.08 at 800nm.

2.6 Materials

Acetone was purchased from Sigma-Aldrich. D3-acetonitirle (CD3CN, 99.5%), and D4-methanol (CD_3OD, 99.8%), were purchased from Cambridge Isotopes. 2-methyl-2-heptene, anhydrous ethanol, dichloromethane (DCM, 99.5%), *N*, *N*-diethyl formamide (DEF, 99.9%), *N*, *N*-dimethylformamide (DMF, 99.9%), yttrium (III) nitrate hexahydrate ($Y(NO_3)_3 \cdot 6H_2O$, 99.9%), and aluminum trichloride hexahydrate ($AlCl_3 \cdot 6H_2O$, 99.9%) were purchased from Fisher Scientific. 3,3-dimethylbutyric acid, manganese nitrate tetrahydrate ($Mn(NO_3)_2 \cdot 4H_2O$), and titanium (IV) isopropoxide were obtained from Alfa Aesar. Lastly, Meso-tetra(4-carboxyphenyl) porphyrin (TCPP, 97%) was purchased from Frontier Scientific. All reagents were used as received without further purification.

CHAPTER 3

The Singlet Oxygen Ene Reaction in Metal-Organic Frameworks: Regiochemistry and Yield

3.1 Materials and Methods:

3.1.1. Photooxidation of 2-Methyl-2-Heptene in MOFs: General Procedure.

We executed the photooxidation of 2-methyl-2-heptene utilizing the MOFs and oxygen supplier under blue LED light. In a glass test tube, we added 15 mol% catalyst loading (based on the porphyrin units in MOFs) in either an aprotic deuterated acetonitrile or a protic deuterated methanol and sonicated the sample for 15minutes. To establish the control group, we utilized a free organic linker, TCPP, instead of MOFs. We also dried our solvents using molecular sieve for the moisture sensitive MOFs. After sonication, we bubbled the oxygen at approximately 1 bubble per second into the sample for 5 minutes and added 0.03mM of 2-methyl-2-heptene. Before radiating the sample, we collected the first sample for ^{1}HNMR to establish the baseline of the reaction. Once the sample had been prepared, we radiated the sample using the blue LED lamps while oxygen was bubbled and collected the samples at 5, 10, 20, and 30 minutes. The DGIST-1 and NUPF-2Y reaction required prolonged radiation. Following the irradiation, samples were analyzed using the ^{1}HNMR. For the reactions in deuterated methanol, we used the intensity of the peak at 4.3ppm (green in Figure 11) and double the intensity to calculate the selectivity due to the methanol peak masking the product 2a peak at 4.9ppm.

To calculate the conversion percentage of the reactant forming to the product, we compared the integral intensity of the reactant peak (Figure 10) with those of two products' integrals (Figures 11 and 12).[10] The conversion percentage was obtained using Equation 1**.** We also calculated the yield ratio using Equation 2.

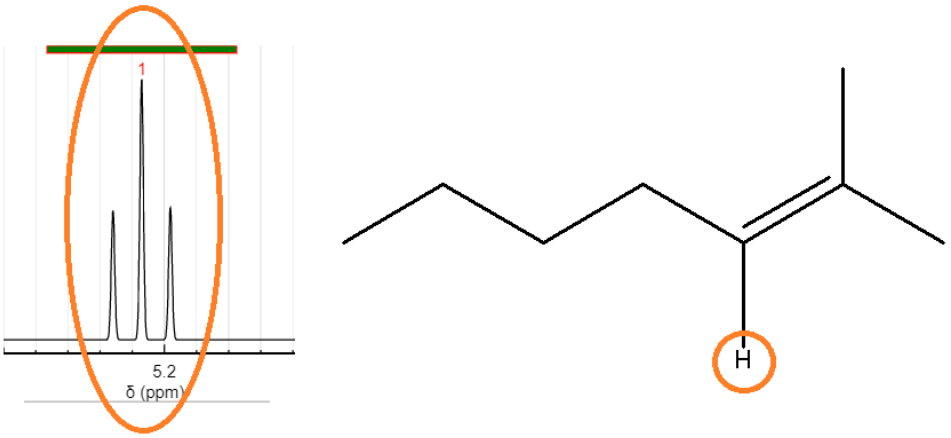


Figure 10. [1]HNMR of reactant 1. The expected peak is a triplet near 5.2ppm.

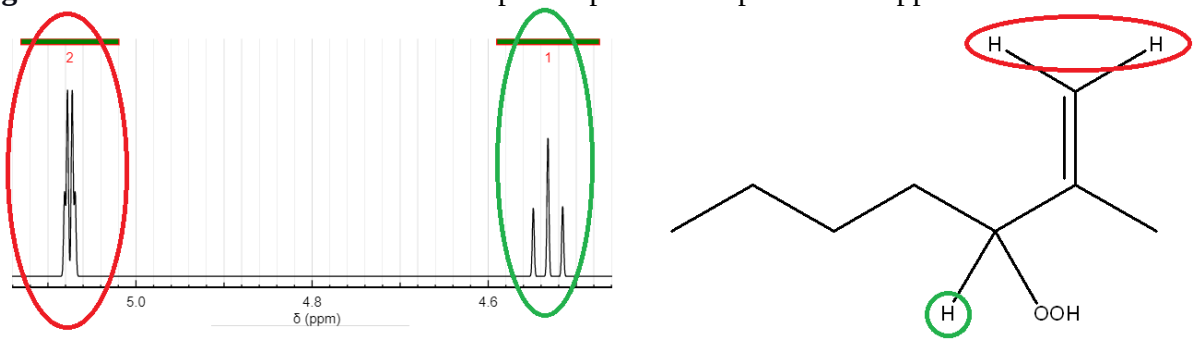


Figure 11. [1]HNMR of product 2a. The expected peaks are a doublet near 5.1ppm and a triplet at 4.5ppm. The intensity of the double (in red) should be twice that of the triplet (in green).

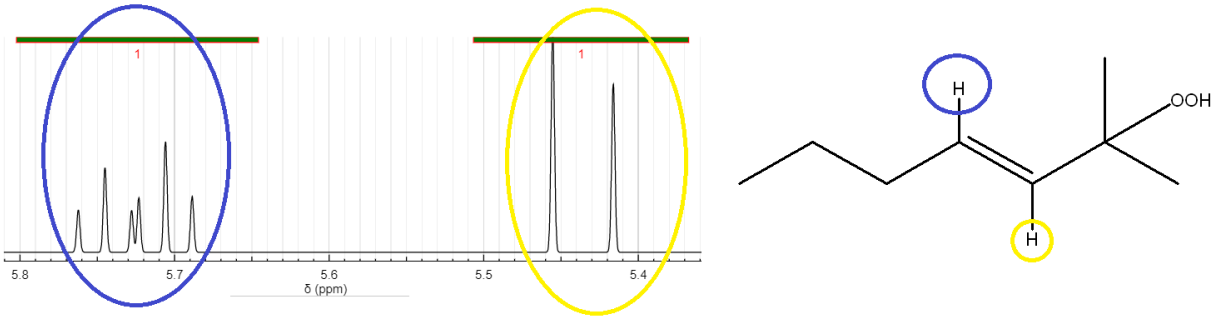


Figure 12. [1]HNMR of product 2b. The expected peak is a doublet of triplet near 5.6ppm. The larger decoupling constant between two peaks confirms the trans configuration of the substrate.

Equation 1. The calculation of conversion percentage using the [1]HNMR data.

$$100\% - \left(\frac{Peak\ Intensity\ of\ Reactant\ (1)}{Peak\ Intensities\ of\ the\ Reactant\ and\ the\ Products\ (2a\ and\ 2b)} * 100\%\right)$$

Equation 2. The calculation of yield ratio using the [1]HNMR data.

$$\frac{Peak\ Intensity\ of\ Product\ 2a}{Peak\ Intensities\ of\ Products\ (2a + 2b)} * 100\%$$

3.1.2 UV-Vis Spectrometer Soret Band

In a glass test tube, we added a small sample of the catalyst and chloroform and sonicated the sample for 5 minutes. After sonication, we diluted the sample until the initial absorbance was between 0.18 and 0.2 at 800nm, then used the UV-vis spectrometer with an integrating sphere to obtain the UV-Vispectra to observe the soret bands of the photosensitizers between 400-450nm; the presence of the soret bands indicates the photosensitizers' ability to generate singlet oxygen under blue LED light.

3.2. Photooxidation of 2-Methyl-2-Heptene in Three Different MOFs: Product Selectivity and Reaction Time.

We carried the photooxidation of 0.03mM solution of 2-methyl-2-heptene in CD_3CN and CD_3OD under a blue LED light. As a control, we first carried out the reaction in the presence of a free organic linker, TCPP. As shown in appendices A and B, the reaction in the aprotic solvent slightly favored product 2a via methyl hydrogen abstraction and required 20 minutes of irritation to complete the reaction. However, carrying out the reaction under the same condition in deuterated methanol slightly favored product 2b via methylene hydrogen abstraction and required 10 minutes to complete the reaction. While experimenting in CD_3OD, we found that the HDO solvent peak masked the product 2a peak near 4.9 ppm. As a result, we chose and doubled the intensity of the peak at 4.3 ppm (green in Figure 11) to calculate the ratio of the products. Lastly, the ^{1}HNMR results showed that the selectivity of both reactions remained consistent throughout the reaction (Appendices A and B).

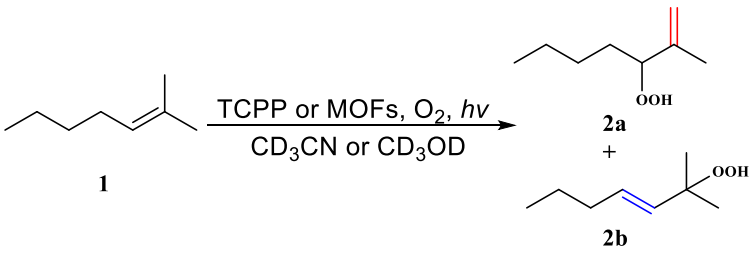


Figure 13. Photooxidation of 0.03mM 2-methyl-2-heptene (1) under blue LED light in CD_3CN or CD_3OD. The reaction in TCPP was recorded as the control group, while the same reaction carried out in MOFs as an experimental group. The bubble rate of the reaction will be 1-2 bubbles per second.

Photosensitizer	Pore Diameter (Å)	Surface Area (m^2/g)	Solvent	2a:2b	Reaction Time
TCPP	NA	NA	CD_3CN	56/44	20mins
Al-TCPP	8.19-9.63	1140-1630	CD_3CN	55/45	30mins
DGIST-1	9.31-9.95	1550-1760	CD_3CN	54/46	150mins
NUPF-2Y	7.98-8.76	1470-1790	CD_3CN	NA	300mins
TCPP	NA	NA	CD_3OD	49/51	10mins
Al-TCPP	8.19-9.63	1140-1630	CD_3OD	49/51	30mins
DGIST-2	9.31-9.95	1550-1760	CD_3OD	NA	NA
NUPF-2Y	7.98-8.76	1470-1790	CD_3OD	NA	150mins

Table 2. Photooxidations of 1 utilizing TCPP and MOFs in deuterated acetonitrile or deuterated methanol. The samples were bubbled at 1-2 bubbles per second and irradiated with a blue LED light. The pore diameter and the surface areas indicate the range of the MOFs synthesized and characterized using PXRD, N2 adsorption, and isotherm. The product ratio was obtained by ^{1}HNMR. The reaction with DIGST-1 was not executed in the deuterated methanol because the framework is sensitive to moisture. Raw ^{1}HNMR are provided in Appendices A-G.

After obtaining the product ratios in a homogenous system, we utilized the MOFs to study the selectivity of the reaction. As shown in Table 2, the results indicated that: while carrying out the reaction with Al and Ti MOFs, product 2a was slightly favored over 2b (product ratio ranged from 54-55) in CD_3CN, whereas the same reactions in CD_3OD slightly favored 2b over 2a. However, the reaction in NUPF-2Y was inconclusive. Although the concentration of the reactant decreased during the reaction, we did not observe the peaks for the products near 4.2ppm, 4.9ppm, and 5.6ppm (Appendices F and G). This study indicates that the confinements of Al-TCPP and DIGST-1 were inadequate to prevent the free rotation of the sigma bond between the carbons in the substrate, resulting in just a minor selectivity change.[10,11,22] However, in the presence of the yttrium MOF, the topology of the MOF may have either: (i) prevented a reactant from entering the pore or (ii) led to different reactions at the active site. In Figure 14, the simulated model indicates that NUPF-2Y has a shp topology, which is denser than those of Al-TCPP and DGIST-1.[23-25] Due to the smaller pore diameter and denser configuration, NUPF-2Y

may have prevented the reactant from entering the inside of the MOF. The results, however, indicated the concentration of the reactant during the reaction without yielding allylic hydroperoxide products, indicating the formation of unknown products.

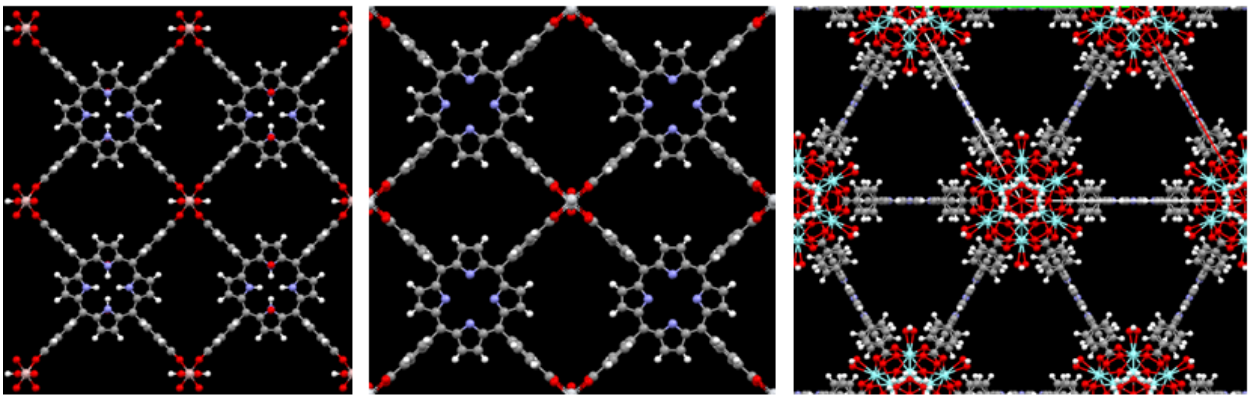


Figure 14. Topology of Al-TCPP, DGIST-1, and NUPF-2Y (from left to right) was obtained using the simulated CIF files from Mercury software. The images indicate that Al-TCPP and DGIST-1 have a ftw configuration while NUPF-2Y has a shp configuration.[23-25]

We also observed that the metal nodes of the MOFs and solvent may affect the reaction time. Once synthesized, the metal nodes in MOFs retain their higher oxidative states. As a result, the electrophilic metal nodes may interact with the nucleophilic oxygen in the perepoxide intermediate. For example, the reaction with DGIST-1 required more extended irradiation than in Al-TCPP. In addition to its smaller pore diameter and denser topology, NUPF-2Y has a denser metal node than that DGIST-1. It is possible that the metal physically quenches singlet oxygen, which could result in a more prolonged reaction. Physical quenching of singlet oxygen by metal complexes has been known for some time,[27-29] but it is currently not known which MOFs (if any) deactivates $^1O_2$.

Lastly, the result illustrated that: while the reactions with TCPP and NUPF-2Y required 20 and 300 minutes of irradiation, respectively, to complete the reaction in CD_3CN, the same reaction in CD_3OD required 10 and 150 mins, respectively. This observation eliminates two crucial factors of solvent effect on: (i) the coordination of metal complex and (ii) the lifetime of

singlet oxygen. Unlike aprotic solvents, deuterated methanol can interfere the coordination of metal via hydrogen bonding and electron-donating oxygen atom,[30] which could prolong the reaction. Furthermore, the lifetime of singlet oxygen in deuterated methanol is shorter than in deuterated acetonitrile.[31-33] However, the reaction in CD_3OD resulted in a shorter reaction time in the homogenous and heterogenous systems. From this observation, we speculate that deuterated methanol may potentially accelerate the reaction by stabilizing the intermediate. During the reaction, the formation of the zwitterionic perepoxide intermediate is the rate-determining step because of the charges on the intermediate. However, in deuterated methanol, the charges on the intermediate can be stabilized via hydrogen bonding and electron donation from the solvent. Such interactions would lower the energy barrier of the reaction and result in a faster reaction in deuterated methanol. However, further investigation is needed to confirm this observation.

CHAPTER 4

Current State of the Singlet Oxygen Ene Chemistry and the Future Direction.

In this study, we performed sensitized photooxidation of 2-methyl-2-heptene utilizing Al-TCPP, DGIST-1, and NUPF-2Y. The result illustrated that utilizing Al-TCPP and NUPF-2Y had a minor effect on the selectivity of the reaction. In contrast, due to its topology and heavy metal nodes, the reaction yielded inconclusive data in the presence of NUPF-2Y. It is possible that the metal nodes in the MOF may physically quench singlet oxygen. Furthermore, we observed that the reaction in deuterated methanol was faster than in deuterated acetonitrile.

Although utilizing MOFs as photocatalysts did not significantly influence the selectivity of the reaction, this study demonstrated the potential of using MOFs for the singlet oxygen ene reaction. Further studies to optimize the overall conditions of the reaction to influence the selectivity are certainly warranted. For future studies, investigating the MOF's topology effect and the singlet oxygen diffusion in the MOFs will improve the overall functionality of the MOFs in the singlet oxygen ene reaction. For example, understanding the topology effect of the MOFs will introduce a physical steric hindrance to control the selectivity of the reaction. Furthermore, studying the diffusion of the singlet oxygen in MOFs can potentially supplement the result in the presence of NUPF-2Y. Although the MOFs had a minor influence on the regiochemistry of singlet oxygen, this study has shown that the various conditions, such as metal nodes, topology, and solvent, of the reaction in MOFs must be studied to maximize the overall utility of the singlet oxygen ene reaction in metal-organic frameworks.

REFERENCES

(1) Ghogare, A. A.; Greer, A. Using Singlet Oxygen to Synthesize Natural Products and Drugs. *Chem. Rev.* **2016**, *116*, 9994–10034.

(2) Bayer, P.; Schachtner, J.; Májek, M.; Jacobi von Wangelin, A. Visible Light-Mediated Photo-Oxygenation of Arylcyclohexenes. *Org. Chem. Front.* **2019**, *6*, 2877–2883.

(3) DeRosa, M. Photosensitized Singlet Oxygen and Its Applications. *Coord. Chem. Rev.* **2002**, *233-234*, 351–371.

(4) G. O. Schenck, H. Eggert and W. Denk, Photochemical reactions. III. The formation of hydroperoxides by the photosensitized reaction of oxygen with appropriate acceptors, especially with α- and β-pinene, *Liebigs Ann. Chem.*, **1953**, *584*, 177–198.

(5) Schweitzer, C.; Schmidt, R. Physical Mechanisms of Generation and Deactivation of Singlet Oxygen. *Chem. Rev.* **2003**, *103*, 1685–1757.

(6) Burgard, A.; Gieshoff, T.; Peschl, A.; Hörstermann, D.; Keleschovsky, C.; Villa, R.; Michelis, S.; Feth, M. P. Optimization of the Photochemical Oxidation Step in the Industrial Synthesis of Artemisinin. *Chem. Eng. J.* **2016**, *294*, 83–96.

(7) Kopetzki, D.; Lévesque, F.; Seeberger, P. H. A Continuous-Flow Process for the Synthesis of Artemisinin. *Chem. Eur. J.* **2013**, *19*, 5450–5456.

(8) Foote, C. S.; Wexler, S. Olefin Oxidations with Excited Singlet Molecular Oxygen. *J. Am. Chem. Soc.* **1964**, *86*, 3879–3880.

(9) Poon, T. H. W.; Pringle, K.; Foote, C. S. Reaction of Cyclooctenes with Singlet Oxygen. Trapping of a Perepoxide Intermediate. *J. Am. Chem. Soc.* **1995**, *117*, 7611–7618.

(10) Vakros, J.; Panagiotou, G.; Kordulis, C.; Lycourghiotis, A.; Vougioukalakis, G. C.; Angelis, Y.; Orfanopoulos, M. [60] Fullerene Supported on Silica and g-Alumina Sensitized Photooxidation of Olefins: Chemical Evidence for Singlet Oxygen and Electron Transfer Mechanism. *Catal. Letters* **2003**, *89*, 269–273.

(11) Li, X.; Ramamurthy, V. Selective Oxidation of Olefins within Organic Dye Cation-Exchanged Zeolites. *J. Am. Chem. Soc.* **1996**, *118*, 10666–10667.

(12) Griesbeck, A. G.; Adam, W.; Bartoschek, A.; El-Idreesy, T. T. Photooxygenation of Allylic Alcohols: Kinetic Comparison of Unfunctionalized Alkenes with Prenol-Type Allylic Alcohols, Ethers and Acetates. *Photochem. Photobiol. Sci.* **2003**, *2*, 877–881.

(13) Guisnet, M.; Ribeiro, F. R. Deactivation and Regeneration of Solid Catalysts. In *Deactivation and Regeneration of Zeolite Catalysts*; IMPERIAL COLLEGE PRESS, 2011; pp 3–18.

(14) Shailaja, J.; Sivaguru, J.; Ramamurthy, V. Zeolite Matrix Assisted Decomposition of Singlet Oxygen Sensitizers during Photooxidation. *J. Photochem. Photobiol. A Chem.* **2016**, *331*, 197–205

(15) Perot, G.; Guisnet, M. Advantages and Disadvantages of Zeolites as Catalysts in Organic Chemistry. *J. Mol. Catal.* **1990**, *61*, 173–196.

(16) Sosa, J.; Bennett, T.; Nelms, K.; Liu, B.; Tovar, R.; Liu, Y. Metal–Organic Framework Hybrid Materials and Their Applications. *Crystals.* **2018**, *8*, 325.

(17) Moosavi, S. M.; Nandy, A.; Jablonka, K. M.; Ongari, D.; Janet, J. P.; Boyd, P. G.; Lee, Y.; Smit, B.; Kulik, H. J. Understanding the Diversity of the Metal-Organic Framework Ecosystem. *Nat. Commun.* **2020**, *11*, 4068.

(18) Alves, S. R.; Calori, I. R.; Tedesco, A. C. Photosensitizer-Based Metal-Organic

Frameworks for Highly Effective Photodynamic Therapy. *Mater. Sci. Eng. C Mater. Biol. Appl.* **2021**, *131*, 112514.

(19) Hynek, J.; Chahal, M. K.; Payne, D. T.; Labuta, J.; Hill, J. P. Porous Framework Materials for Singlet Oxygen Generation. *Coord. Chem. Rev*. **2020**, *425*, 213541.

(20) Sreehari Surendran, R.; Xinlin, L.; Pravas, D. Physical Properties of Porphyrin-Based Crystalline Metal–organic Frameworks. *Commun. Chem.* **2021**, *4*, 47.

(21) Yu, W.; Zhen, W.; Zhang, Q.; Li, Y.; Luo, H.; He, J.; Liu, Y. Porphyrin-Based Metal-Organic Framework Compounds as Promising Nanomedicines in Photodynamic Therapy. *ChemMedChem* **2020**, *15*, 1766–1775.

(22) Hemmer, K.; Cokoja, M.; Fischer, R. A. Exploitation of Intrinsic Confinement Effects of MOFs in Catalysis. *ChemCatChem* **2021**, *13*, 1683–1691.

(23) Arriaga Gomez. J.C. Optimization of Porphyrin-Based Metal-Organic Frameworks for Selective Oxidation of Organic Sulfieds, Master of Science Thesis, California State University, Los Angeles, CA, 2022

(24) Fateeva, A.; Chater, P. A.; Ireland, C. P.; Tahir, A. A.; Khimyak, Y. Z.; Wiper, P. V.; Darwent, J. R.; Rosseinsky, M. J. A Water-Stable Porphyrin-Based Metal-Organic Framework Active for Visible-Light Photocatalysis. *Angew. Chem. Int. Ed Engl.* **2012**, *51*, 7440–7444.

(25) Keum, Y.; Park, S.; Chen, Y.; Park, J. Titanium-Carboxylate Metal-Organic Framework Based on an Unprecedented Ti-Oxo Chain Cluster. *Angew. Chem. Int. Ed.* **2018**, *57*, 14852-14856.

(26) Xu, L.; Zhai, M.-K.; Wang, F.; Sun, L.; Du, H.-B. A Series of Robust Metal–Porphyrinic Frameworks Based on Rare Earth Clusters and Their Application in N–H Carbene Insertion. *Dalton Trans.* **2016**, *45*, 17108–17112.

(27) Hernandez, B.; Wang, Y.; Zhang, D.; Selke, M. Photooxidation of Co-Thiolato Complexes in Protic and Aprotic Solvents. *Chem. Commun.* **2006**, *9*, 997.

(28) Selke, M. Reactions of Metal Complexes with Singlet Oxygen. *PATAI'S Chemistry of Functional Groups*; John Wiley & Sons, Ltd: Chichester, UK, 2014; pp 1–50.

(29) Carlsson, D. J.; Mendenhall, G. D.; Suprunchuk, T.; Wiles, D. M. Singlet Oxygen ($^1\Delta_g$) Quenching in the Liquid Phase by Metal (II) Chelates. *J. Am. Chem. Soc.* **1972**, *94*, 8960–8962.

(30) Khentov, V.; Semchenko, V. V.; Hussein, H. H. H. Increasing the Rate of the Direct Synthesis Complex Compounds. In *Direct Synthesis of Metal Complexes*; Elsevier, 2018; pp 279–313.

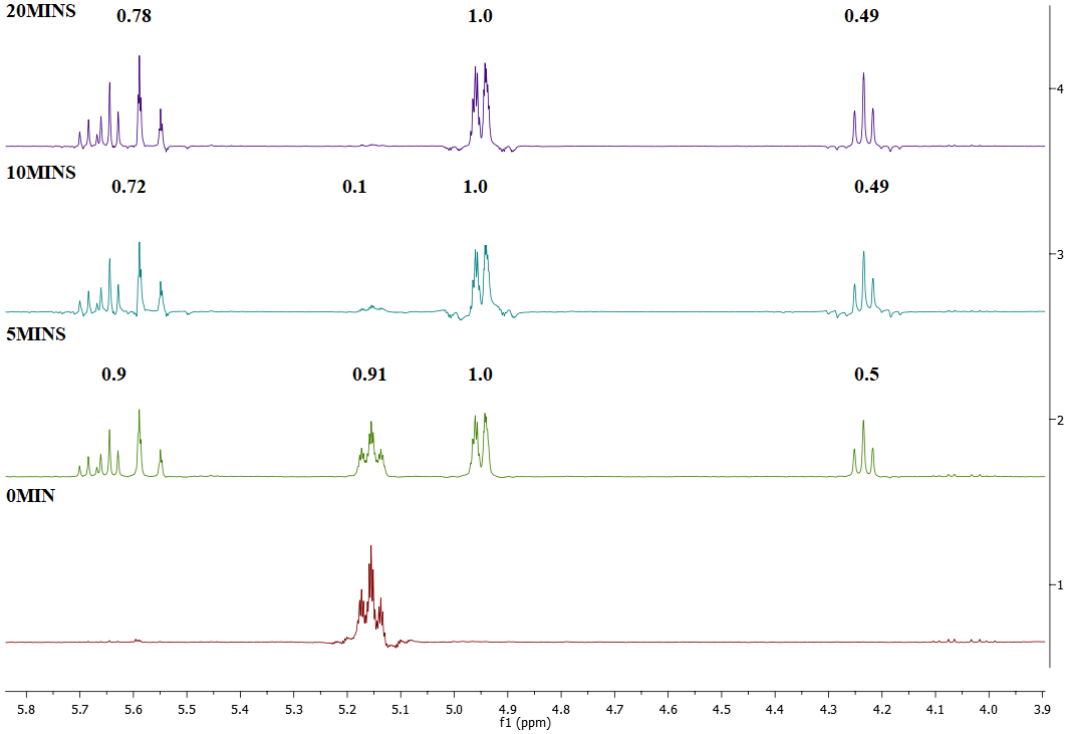
(31) Lemp, E.; Pizarro, N.; Encinas, M. V.; Zanocco, A. L. Solvent Effect on the Quenching of Singlet Oxygen by 3-Methylindole. *Phys. Chem. Chem. Phys.* **2001**, *3*, 5222–5225.

(32) Ogilby, P. R.; Foote, C. S. Chemistry of Singlet Oxygen. 42. Effect of Solvent, Solvent Isotopic Substitution, and Temperature on the Lifetime of Singlet Molecular Oxygen ($^1\Delta_g$). *J. Am. Chem. Soc.* **1983**, *105*, 3423–3430.

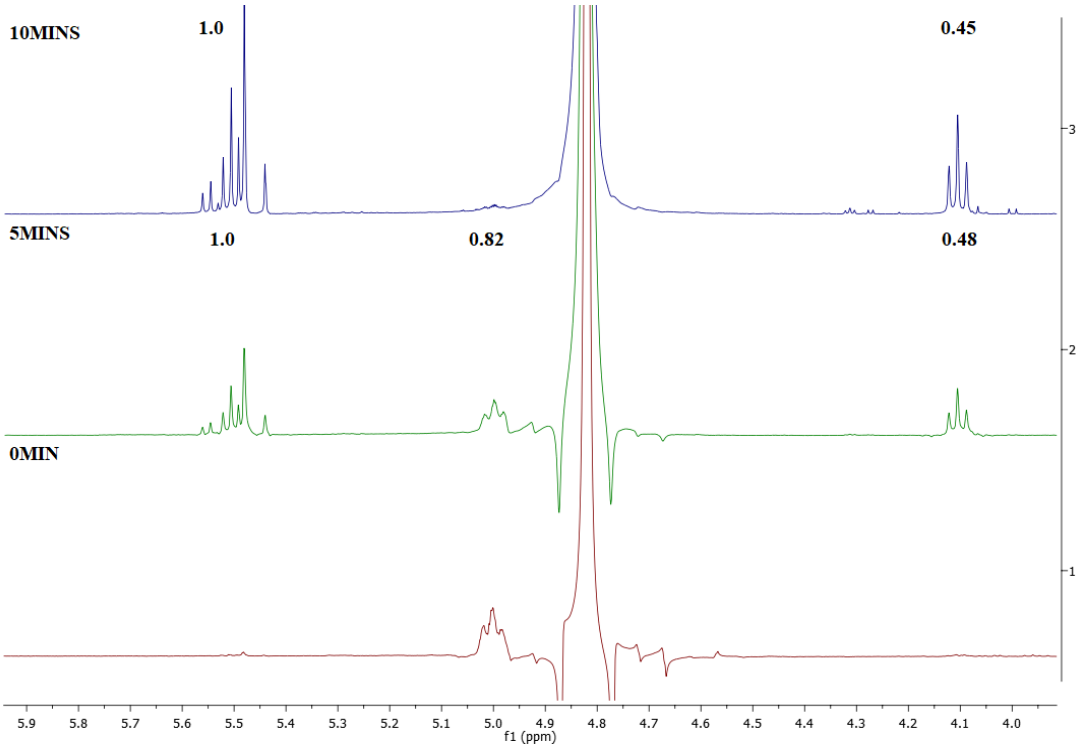
(33) Chacon, J. N.; McLearie, J.; Sinclair, R. S. Singlet Oxygen Yields and Radical Contributions in the Dye-Sensitised Photo-Oxidation in Methanol of Esters of Polyunsaturated Fatty Acids (Oleic, Linoleic, Linolenic and Arachidonic). *Photochem. Photobiol.* **1988**, *47*, 647–656.

APPENDICES

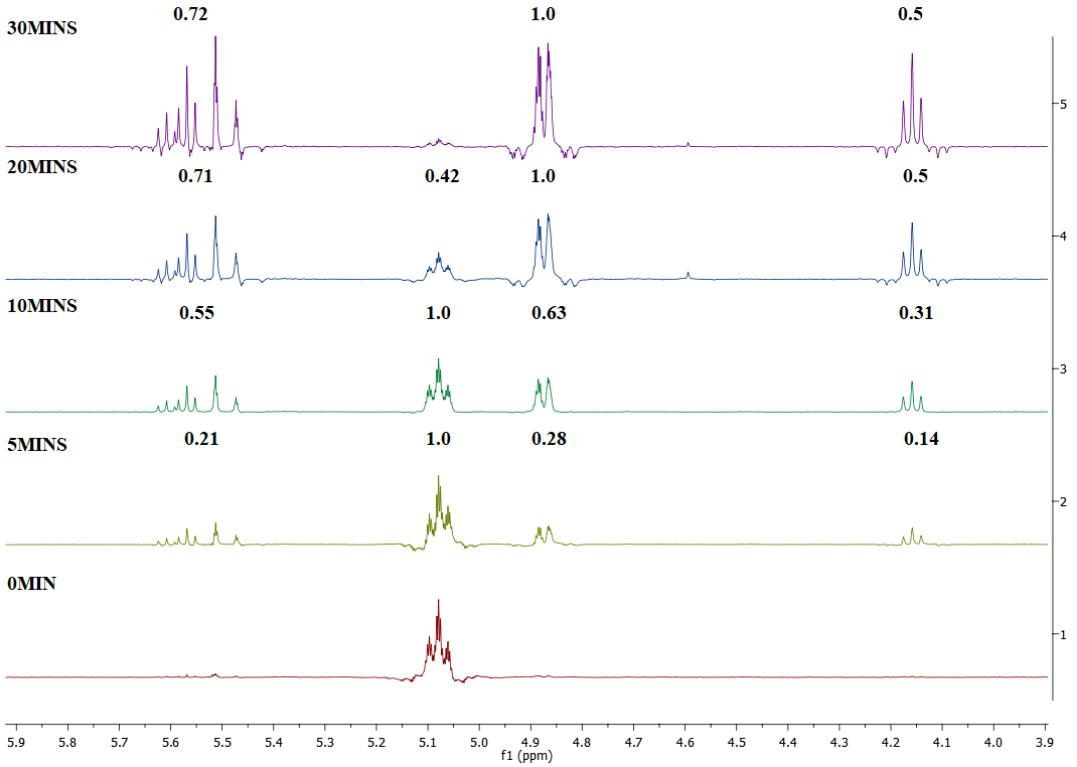
Appendix A. ^{1}HNMR of photooxidation with TCPP in CD_3CN



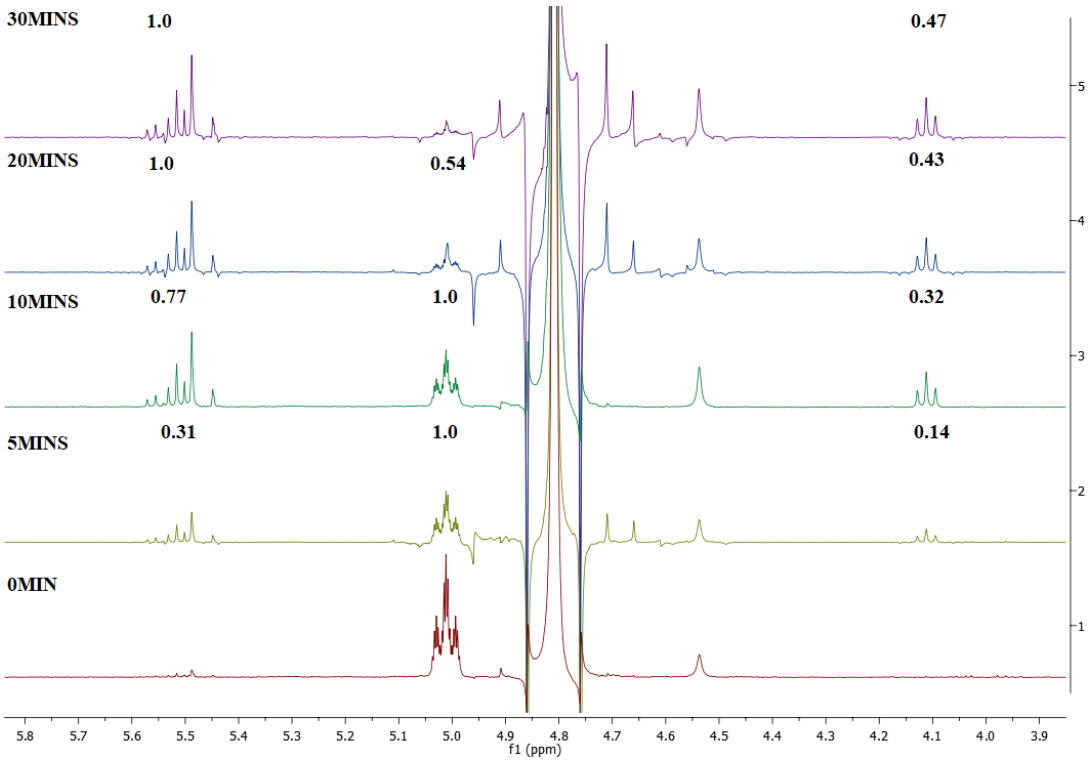
Appendix B. ^{1}HNMR of photooxidation with TCPP in CD_3OD



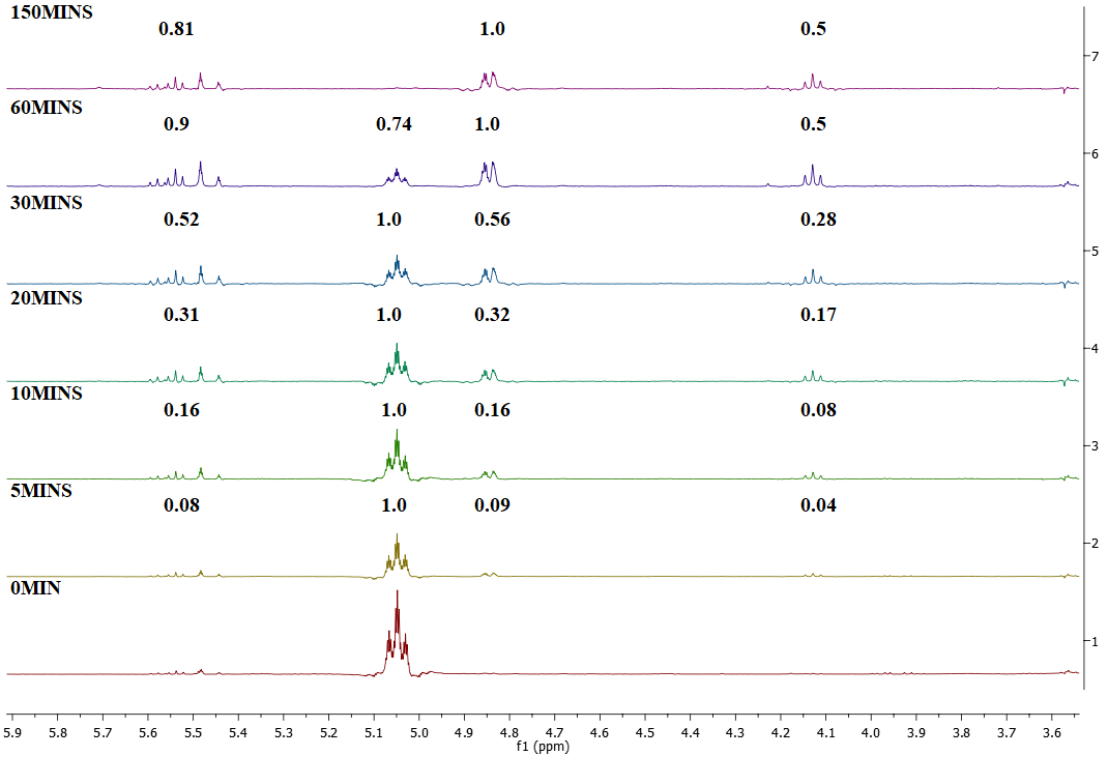
Appendix C. ^{1}HNMR of photooxidation with Al-TCPP in CD_3CN



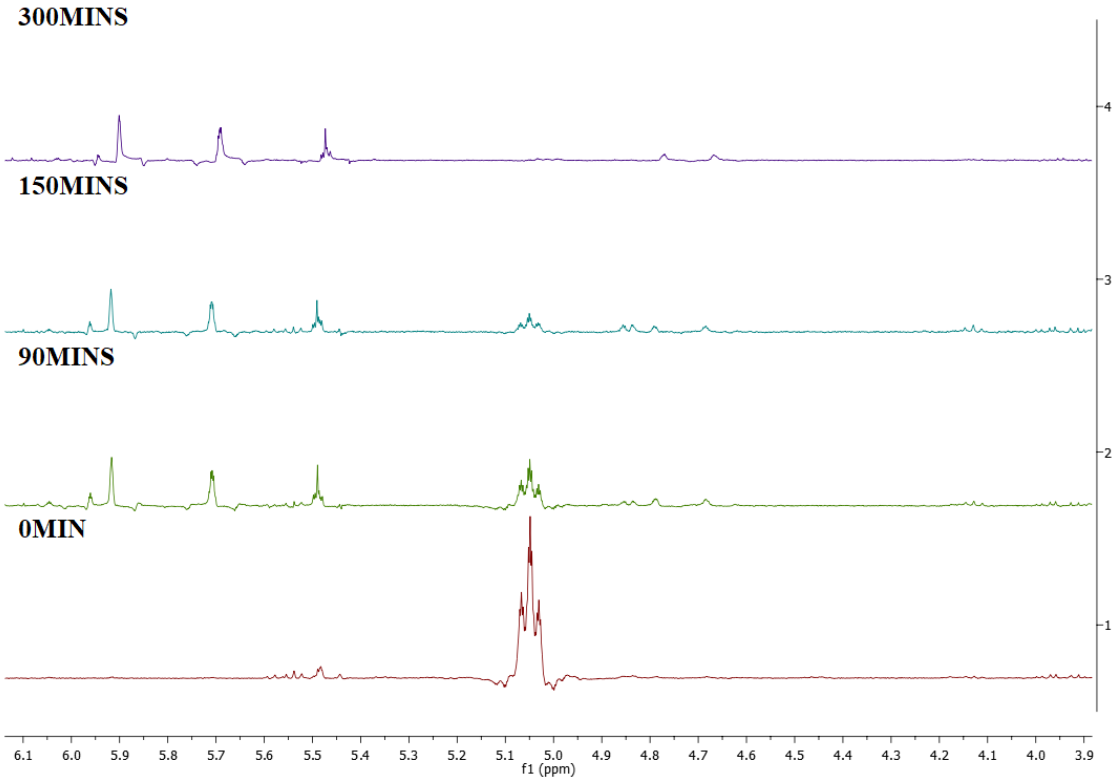
Appendix D. ^{1}HNMR of photooxidation with Al-TCPP in CD_3OD



Appendix E. ^{1}HNMR of photooxidation with DGIST-1 in CD_3CN



Appendix F. ^{1}HNMR of photooxidation with NUPF-2Y in CD_3CN



Appendix G. ^{1}HNMR of photooxidation with NUPF-2Y in CD_3OD

